Vol 13 No 6, June 2004
1009-1963/2004/13(06)/0891-07

Chinese Physics

© 2004 Chin. Phys. Soc.
and IOP Publishing Ltd

Emission spectra simulation of calcium plasmas in non-local thermodynamic equilibrium*

Liang Gui-Yun(梁贵云), Bian Xia(边 霞), and Zhao Gang(赵 刚)

National Astronomical Observatories, Chinese Academy of Sciences, Beijing 100012, *China*

(Received 19 August 2003; revised manuscript received 7 January 2004)

We use previous high-quality experimental spectra to test the accuracy of atomic data and the validity of the collisional–radiative (CR) model used in this paper. The synthetic spectrum with electron temperature $\log T_e(\mathrm{K})=6.745$ and electron density $n_e=6.0\times10^{13}\,\mathrm{cm}^{-3}$, which almost reproduces the experimental spectra, is presented. Nearly all the features of the experimental spectra were identified. The results of the CR modelling for the emission spectra of calcium plasmas all agree well with the measured spectral line intensities within the experimental error for most of the lines. Furthermore, we make the electron temperature diagnostic through the synthetic spectrum and population fractions of every ionization state as a function of charge state at different electron temperatures, as well as the electron density diagnostic through the intensity ratios of two lines of Be-like calcium and three lines of C-like calcium. A good agreement between the calculated values and the measured ones is found.

Keywords: atomic process, plasma, electron temperature and density diagnostic, spectra
PACC: 5225P, 5270

1. Introduction

The questions about the temperature of coronal flare plasma, electron density measurements, non-equilibrium processes and relative element abundances are still unresolved. The new generation of x-ray satellites (Chandra, XMM-Newton) enables us to obtain spectra of stars with unprecedented high spectral resolution and high signal-to-noise (S/N) ratio, which will help us to reduce these problems. Many unresolved emission lines in the past can be resolved through the Chandra mission, especially the weak satellites of lithium-like ions blended with strong helium-like triplets from C V to Si XIII which have the diagnostic potential for electron densities ($n_e \approx 10^8 - 10^{13}\,\mathrm{cm}^{-3}$) as well as electron temperatures ($T_e \approx (1-6)\times10^6\,\mathrm{K}$). Moreover, the line intensity ratios of these He-like triplets enable also the determination of the ionization processes (photo-ionization and/or collision-ionization) which prevail in the astrophysical plasmas.[1,2] However, the principal work of developing the above-mentioned problems is the calculation of line intensities. The line intensities can be determined from level populations and radiative transition probabilities. In order to obtain the level populations, different models and assumptions have been adopted to account for the atomic processes occurring in the plasma. Basically, they can be classified into the local thermodynamic equilibrium (LTE) and non-LTE plasma models. Recently, Zeng *et al*[3–5] have studied the absorption spectra of plasmas in LTE by using a detailed-term-accounting model. Their theoretical simulations show an excellent agreement with the experiments. In solar, stellar corona and some laboratory tokamak plasmas, however, the hot and low-density plasmas are often in non-LTE. In non-LTE plasmas, the level populations are obtained through solving coupled rate equations, in which a lot of atomic data such as energy levels, radiative transition probabilities and electron impact excitation cross sections are required. As Doschek[6] pointed out, the atomic physics plays a crucial role for this kind of plasma diagnostics.

Calcium is an abundant element in astrophysical objects. It attracts many astrophysicists to investigate the electron temperature and density of astrophysical plasmas using electron temperature-sensitive and electron density-sensitive lines of calcium. For that, the calculation of electron impact excitation rates is essential to infer reliable electron temperatures and

*Project supported by the Special Foundation for State Major Basic Research Programme of China (Grant No G1999075406) and the National Natural Science Foundation of China (Grant No 10373014).

densities of astrophysical and experimental plasmas. At present, most data of electron collisions were calculated by using the distorted wave approximation. Although a more accurate result can be obtained by using a relativistic R-matrix method, it needs more time and computer resources. In 1998, Keenan *et al*[7] recalculated the electron impact excitation rates of Ca XVI by using this method, derived electron density-sensitive ratios involving $2s^2 2p$–$2s 2p^2$ of Ca XVI with the new electron impact excitation rates data, and compared them with the observational values of the solar flares. A close agreement was obtained between the theoretical calculation and the observation. In the same year, Kato *et al*[8] first derived the emission measure from He-like Ca XIX ion and Fe XXV spectra without assuming the ionization equilibrium and solar abundance when studying the solar flare spectra. In Ref.[8], the authors concluded that the flare plasma is a time-dependent, non-equilibrium ionizing plasma from ion density ratios. In the rising phase of the flare plasma, blue-shifts of the calcium lines make the line widths broader; the ion temperatures are derived from the broadening of the resonance line of the Ca XIX. In laboratory, Lippmann *et al*[9] first measured the line brightness ratios using the TEXT tokamak facility and modelled the calcium plasma spectra with the wavelengths covering the range of 14–22 nm. In Ref.[9], the atomic data used were very limited with the maximum main quantum number only n=2. In addition, the authors pointed out the importance of the inclusion of the $2p^{k+2}$ levels of calcium ions. In 2000, Soukhanovskii *et al*[10] re-analysed the experimental spectra of highly ionized calcium using the more accurate atomic data calculated by Hebrew University-Lawrence Livermore Atomic Code (HULLAC), and modelled the calcium plasma by using the HULLAC package. In Ref.[10], the authors made a detailed analysis, even the levels of main quantum number n=4 and 5 were included. They found that the effect of radiative cascades on the population n=2 levels from n=4, 5 was less than 5%. In addition, they presented the relative intensities of lines and the level population relative to the ground level for individual calcium ions with the maximum abundance, and diagnosed the electron temperature using the line intensity ratio of the Be-like calcium ion. As to special experimental spectra of calcium plasma, the simulation of emission spectra [11,12] and the determination of electron temperature and density of the plasma have not been given yet.

In order to test the completeness and accuracy of the atomic database and the validity of the collisional–radiative (CR) model used in the present paper, we simulate the emission spectra of calcium plasma produced at the TEXT tokamaks by Lippmann *et al.*[9] Moreover, we calculate the line intensities of individual ions at the logarithmic electron temperature $\log T_e(\mathrm{K})$=6.745 and the electron density n_e=6.0×10^{13} cm^{-3}, and provide theoretical spectra of calcium plasmas which almost reproduce the experimental spectra. Through comparison with experimentally measured relative intensities of lines, we find that the results of our CR modelling for the emission spectra of calcium plasmas agree very well within the experimental error bars for most lines. In addition, we further make the electron temperature diagnostics through the synthetic spectrum and the electron density diagnostic through the intensity ratio of two lines of Be-like calcium, $R_1 = \dfrac{I(2s2p\ ^1P_1 - 2s^2\ ^1S_0)}{I(2p^2\ ^3P_2 - 2s2p\ ^3P_2)}$, and the ratios between three lines of C-like calcium, $R_2 = \dfrac{I(2s2p^3\ ^1D_2 - 2s^2 2p^2\ ^1D_2)}{I(2s2p^3\ ^3P_0 - 2s^2 2p^2\ ^3P_1)}$ and $R_3 = \dfrac{I(2s2p^3\ ^1D_2 - 2s^2 2p^2\ ^1D_2)}{I(2s2p^3\ ^3P_1 - 2s^2 2p^2\ ^3P_1)}$. A good agreement between the calculated values and the measured ones was found.

This paper is organized as follows: the detailed theoretical method is described in Section 2; results and discussion are presented in the last section.

2. Theoretical methods

The line intensity (phot·cm^{-3}s^{-1}) of a specific spectral line transition $j \to i$ is given by

$$I_{j,i}(\lambda) = N_j(X^{+m}) A_{j,i} S(\lambda), \tag{1}$$

where $A_{j,i}$ (s^{-1}) is the Einstein spontaneous emission coefficient (A value); $N_j(X^{+m})$ is the number density of the level j of the ion X^{+m}; $S(\lambda)$ is the line shape function. In the present work, a Gaussian profile is assigned to it,

$$S(\lambda) = \frac{\sqrt{\ln 2}}{\sqrt{\pi}\Gamma} \mathrm{e}^{\ln 2(\lambda-\lambda_0)^2/\Gamma^2}, \tag{2}$$

where λ_0 is the wavelength of the transition, and 2Γ is the spectral resolution of the spectrometer.

The number density population of level j of a non-LTE plasma is obtained through solving a set of coupled rate equations. In principle, the rate equations should include all of the collisional excitations,

de-excitations and the radiative decays between all fine-structure levels of each ionization stage as well as other atomic processes. The present model ignores the contribution from the ionization and recombination processes. And the main quantum number n is cut at $n = 3$. The electron energy distribution is assumed to be Maxwellian, corresponding to an electron temperature T_e. The set of rate equations for the (time dependent) number density $N_j(X^{+m})$ in ions with charge $+m$ in a level j can be written as

$$\frac{\mathrm{d}}{\mathrm{d}t}N_j(X^{+m}) = N_e\sum_{i\neq j} C_{i,j}N_i(X^{+m}) + \sum_{i>j} A_{i,j}N_i(X^{+m}) - N_j(X^{+m}) \times \left(N_e\sum_{i\neq j} C_{i,j} + \sum_{i<j} A_{j,i}\right), \quad (3)$$

where $C_{i,j}$ is the electron impact excitation rate coefficient. If we assume a steady state, i.e. $\mathrm{d}N_j/\mathrm{d}t=0$, Eq.(2) reduces to a set of linear algebraic equations. The collisional excitation rate for a Maxwellian electron velocity distribution can be expressed as [1,9]

$$C_{i,j} = \frac{8.63\times10^{-6}}{T_e}\frac{\Upsilon_{i,j}(T_e)}{\omega_i}\exp\left(-\frac{\Delta E_{i,j}}{kT_e}\right), \quad (4)$$

where ω_i is the statistical weight of level i, k is the Boltzmann constant and $\Upsilon_{i,j}$ is the thermally-averaged collision strength (effective collision strength):

$$\Upsilon_{i,j} = \int_0^\infty \Omega_{i,j}\exp\left(-\frac{E}{kT_e}\right)\mathrm{d}\frac{E}{kT_e}. \quad (5)$$

Here $\Omega_{i,j}$ is the electron collision strength, which is a function of incident electron energy. E is the colliding electron kinetic energy after excitation has occurred.

The corresponding de-excitation is given by [13]

$$C_{j,i} = \frac{\omega_i}{\omega_j}\exp\left(\frac{\Delta E}{kT_e}\right)C_{i,j} \qquad j > i, \quad (6)$$

where ΔE is the positive energy separation of levels i and j.

The number density can be obtained by solving the set of Eq.(2) with the sum of all level populations to total number density of that ion $\left(\sum_j N_j(X^{+m}) = N(X^{+m})\right)$. In this paper, we use the collisional ionization balance calculated by Mazzotta *et al*[14] because it is a recent compilation.

The energy levels, Einstein spontaneous emission coefficient $A_{j,i}$ (s^{-1}), and the electron collision strength $\Omega_{i,j}$ or effective collision strength $\Upsilon_{i,j}$ needed to solve Eq.(2) are available in the literature. The corresponding configurations considered in our model are up to main quantum number n=3. Here, we briefly describe the configurations of high population fractional ions and the data sources of energy levels, oscillator strength and A values as well as collision strength. Detailed illustrations are provided in Refs.[15] and [16] (and references therein). All the experimental energy levels of Ca XVIII–XII are from the NIST database. The theoretical energy levels are obtained from some available reference papers. For lithium-like calcium, configurations $1s^2nl$ (n=2, l=s, p; n=3, l=s, p, d; n=4, l=s, p, d, f; n=5, l=s, p, d, f, g), $1s2s^2$, $1s2s2p$, $1s2p^2$ are considered. The oscillator strengths used in the present paper are provided by Zhang *et al*[17] and Martin *et al.*[18] The present paper adopts relativistic distorted wave (DW) collision strengths calculated by Zhang *et al.* For beryllium-like calcium, our model includes 46 levels of the configurations $2s^2$, $2p^2$, 2s2p, 2s3l (l=s, p, d), 2p3l (l=s, p, d). Zhang and Sampson [19] provided electric dipole oscillator strength and A values for all the allowed transitions. The collision strengths used in the present paper are provided by Zhang *et al*, who adopted the relativistic DW method. For boron-like calcium, 125 levels of the configurations $2s^22p$, $2s2p^2$, $2p^3$, 2s2p3l (l=s, p, d), $2s^23l$ (l=s, p, d), $2p^23s$ and $2p^23d$ are included. Oscillator strengths and A values for the n=2 levels were obtained from Ref.[20]. For n=3 levels, the oscillator strengths were obtained from the unpublished calculations of Zhang and Sampson[1)] . The effective collision strengths for n=2 levels were from Zhang's work which adopted R-matrix calculations. For n=3 levels, we use the collision strength calculated by Zhang and Sampson using the Coulomb–Born method. For carbon-like calcium, the configurations $2s^22p^2$, $2s2p^3$, $2p^4$ and $2s^22p3l$ (l=s, p, d) are included in our model of 46 levels. The collision strengths are provided by Bhatia and Doschek.[21] For nitrogen-like calcium, 15 levels of the configuration $2s^22p^3$, $2s2p^4$ and $2p^5$ are included. The consideration of the configuration $2p^5$, which has not been considered in the HULLAC calculation, improves the accuracy of calculations. For oxygen-like calcium, the configurations $2s^22p^4$, $2s2p^5$,

[1)] Zhang H L and Sampson D H 1995 unpublished work (private communication).

$2p^6$ and $2s^22p^33s$ are included in our model of 20 levels. The radiative transition probabilities and the collision strengths are taken from the calculations of Bhatia and Mason.[22] The configuration $2p^3$ of B-like ion and the configuration $2p^4$ of C-like ion are also included in our model. These two configurations are important for improving the theoretical prediction accuracy, which has been pointed out by Lippmann *et al.*[9] In addition, the configuration $2p^5$ of N-like ion of calcium has also been considered in the present calculation.

The experimental spectral data come from the experiment conducted at the TEXT tokamaks. The details of the experiment has been described by Lippmann *et al*[9] and Finkenthal *et al.*[23] The experiment was conducted at the electron temperature of 1 keV and the electron density of $3.5\times10^{13}\,\mathrm{cm}^{-3}$. But the injection of CaF_2 causes the electron temperature decreases by 25%, while the electron density increases by 18%.

3. Results and discussion

The theoretical spectra at different electron temperatures and the experimental spectrum of highly ionized calcium plasma in the wavelength range 5–35 nm are presented in Fig.1. The Gaussian profile was adopted to fit the experimental spectral line. The corresponding full width at half maximum is the instrumental spectral resolution $\Delta\lambda = 0.08$ nm. In this wavelength range, most lines come from the electron-impact-excited transitions $\Delta n = 0$. In the top panel, we give the synthetic spectra with the logarithmic electron temperature $\log T_e(\mathrm{K})=6.745$ and electron density $6.0\times10^{13}\,\mathrm{cm}^{-3}$ in collisional ionization balance. The parameters are the most optimized values. The optimized electron temperature is obtained through many times of comparison between the theoretical line intensities and the measured ones when changing the electron temperature with the electron density fixed; then inversely, the electron temperature is fixed, adjusting the electron density, until the optimized electron density is obtained in this loop; then again adjusting the electron temperature, until the optimized electron temperature is obtained in the loop. After many repeating these processes many times, the optimized electron temperature ($\log T_e(\mathrm{K})=6.745$) and density ($6.0\times10^{13}\,\mathrm{cm}^{-3}$) are obtained, which are consistent with the experiment-measured values $\log T_e(\mathrm{K})=6.875$ and $5.1\times10^{13}\,\mathrm{cm}^{-3}$ respectively. Comparison with the experimental spectra shown in Fig.1(b), shows that the theoretical spectra almost completely reproduce the experimental spectra. From Fig.1(a), we can see that all the strong lines and relatively weak lines from calcium ions are identified and fitted very well, except that some weak lines between the wavelength range 31–34 nm do not appear, since they are from the electron impact excitation of fluorine ions. In Fig.1(b), the electron transition of some strong lines are also labelled in the panel. In addition, we present the measured and calculated relative line intensities of some strong lines in Table 1. Measured and calculated relative intensities (rel. int.) of some strong lines of calcium ions are normalized to the strongest resonance line $2s2p\ ^1P_1$–$2s^2\ ^1S_0$ (19.29 nm) of Ca XVII. The present calculated relative intensity values are listed in the last column. The measured relative brightness of the two lines widely separated in wavelength was

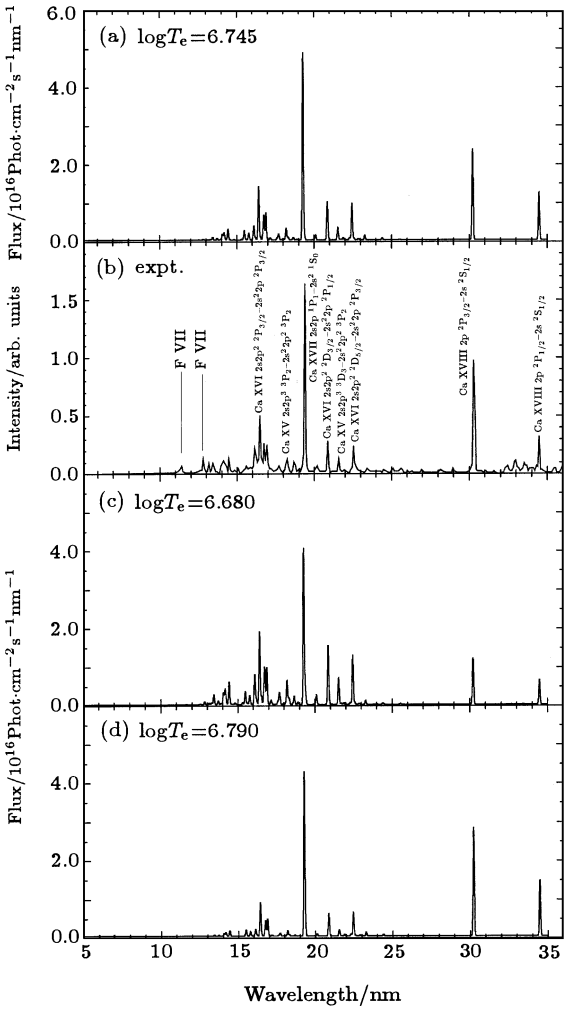


Fig.1. Theoretical spectra with electron density $6.0\times10^{13}\,\mathrm{cm}^{-3}$ and different electron temperatures and experimental spectrum of highly ionized calcium in the TEXT tokamak.

estimated to be $\leq$20%, which has been pointed out in Ref.[9]. The measured error will be larger than this value for those blended lines. From the last two columns, we can see that the present calculated results are all in agreement with the measured values within the experimental error. This indicates that the CR model used in the present paper is valid and the atomic data including n=2 and n=3 configurations are adequate to predict L-shell line intensities. However, the relative line intensities of λ=30.22 and 34.48 nm of Li-like calcium have large deviations between the present calculation ($\sim$ 1.9) and the experimental measurement ($\sim$ 3). This is attributed to the calibration uncertainty of the measurements (above 30 nm), which has been pointed out in the paper published by Lippmann *et al.*[9]

Table 1. Measured and calculated relative intensities (rel. int.) of some strong lines of calcium ions.

Ions	Lower level	Upper level	λ/nm	Measured	Present
Ca XVIII	2s $^2S_{1/2}$	2p $^2P_{3/2}$	30.22	59.57	48.32
Ca XVIII	2s $^2S_{1/2}$	2p $^2P_{1/2}$	34.48	19.86	25.02
Ca XVII	2s^2 $^1S_0$	2s2p $^1P_1$	19.29	100	100
Ca XVI	2s^{2}2p $^2P_{3/2}$	2s2p^2 $^2P_{3/2}$	16.42	31.20	28.51
Ca XVI	2s^{2}2p $^2P_{3/2}$	2s2p^2 $^2P_{1/2}$	16.74	16.31	13.58
Ca XVI	2s^{2}2p $^2P_{1/2}$	2s2p^2 $^2S_{1/2}$	16.89	15.60	14.30
Ca XVI	2s^{2}2p $^2P_{1/2}$	2s2p^2 $^2D_{3/2}$	20.86	17.73	20.17
Ca XVI	2s^{2}2p $^2P_{3/2}$	2s2p^2 $^2D_{5/2}$	22.46	14.89	19.54
Ca XV	2s^{2}2p^2 $^1D_2$	2s2p^3 $^1D_2$	16.10	13.47	7.53
Ca XV	2s^{2}2p^2 $^3P_1$	2s2p^3 $^3P_1$	17.69	4.24	3.24
Ca XV	2s^{2}2p^2 $^3P_2$	2s2p^3 $^3P_2$	18.19	7.60	6.13
Ca XV	2s^{2}2p^2 $^3P_2$	2s2p^3 $^3D_3$	21.54	7.80	6.71

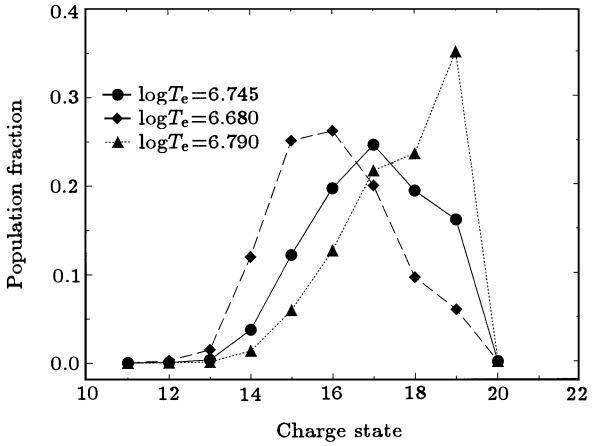


Fig.2. Population fractions of every ionization state versus charge state for calcium plasma with an electron density 6.0×10^{13} cm^{-3} at different electron temperatures.

In order to diagnose the electron temperature of plasma, we also present the theoretical spectra with another two typical different electron temperatures in Fig.1. Figures 1(a), (c) and (d) show that the synthetic spectra are very sensitive to electron temperature. The intensity ratios of lines with λ=30.22 and 34.48 nm of Ca XVIII to the line with λ=20.87 nm of Ca XV and to the lines with λ=21.88 and 22.46 nm of Ca XVI clearly indicate this point in Fig.1. With the increase of electron temperature, the ratios also increase from $\sim$ 0.9 to 2–3. This is mainly due to the sensitivity of distribution of every ionization stage of calcium to the electron temperature, which is shown clearly through the population fraction of every ionization stage versus the charge state at different electron temperatures as shown in Fig.2. At the logarithmic electron temperature $\log T_e$=6.680, Ca XVI has the maximum fraction $\sim$27%. When the logarithmic electron temperature ascends to 6.790, the fraction of Ca XVI falls to only $\sim$13%, while the fraction of Ca XIX increases from $\sim$6% to $\sim$36%.

In general, the sensitivity of spectra to electron density is not similar to that of spectra to electron temperature. The intensity ratio of two $\Delta n = 0$ lines of the same ion which is sensitive to the electron density can usually be used as a tool for diagnosing electron density of plasmas. Particular attention has been paid to Be-like calcium since its use as a solar flare diagnostic was pointed out by Doschek.[6] Upper levels of both λ=19.28 and 23.28 nm lines of Be-like calcium are populated by electron impact excitation.

The upper level 2s2p $^1P_1$ of the strong resonance line is populated from the ground state, whereas the upper level $2p^2$ of a weak line is populated from the ground state and from the 2s2p ^3P levels. The upper level of the two lines are strongly coupled through electron collision. Therefore, the brightness ratio between this weak line and the resonance line can be used to diagnose the electron density of the plasma, and this ratio has been widely applied to diagnose electron density of the solar flare spectrum. For the C-like ion, it has a multilevel ground configuration, in this case $2s^22p^2\ ^3P$. The excited configuration is triplet levels $2s2p^3\ ^3P$. Between the levels of a multilevel configuration, the electron impact excitation greatly affects the population of every sub-level. Therefore, we use the intensity ratio between two lines of Be-like calcium, $R_1 = \dfrac{I(2s2p^1P_1 - 2s^2\ ^1S_0)}{I(2p^2\ ^3P_2 - 2s2p\ ^3P_2)}$, and the ratios between three lines of C-like calcium, $R_2 = \dfrac{I(2s2p^3\ ^1D_2 - 2s^22p^2\ ^1D_2)}{I(2s2p^3\ ^3P_0 - 2s^22p^2\ ^3P_1)}$ and $R_3 = \dfrac{I(2s2p^3\ ^1D_2 - 2s^22p^2\ ^1D_2)}{I(2s2p^3\ ^3P_1 - 2s^22p^2\ ^3P_1)}$ to determine the range of electron density of the experimental plasma. The result is shown in Fig.3. The measured intensity ratios of R_1, R_2 and R_3 are 50, 5 and 3.18 respectively, which are denoted by filled circles with 20% error bars in the figure. The corresponding ranges of electron density are $\sim 3.0\times10^{12} - 3.5\times10^{14}$ cm^{-3}, $\sim 2.0\times10^{13} - \geq 10^{15}$ cm^{-3} and $\sim 9.0\times10^{12} - 6.7\times10^{13}$ cm^{-3}, respectively. But the overlap of these three ranges, indicated by two vertical long dashed lines, is a narrower range $\sim 2.0\times10^{13} - 6.7\times10^{13}$ cm^{-3}, which is shown clearly in the three panels of Fig.3. The synthetic spectra with the electron density within this range can reproduce the laboratory spectra well, and the derived range of electron density is consistent with the measured value of 5.1×10^{13} cm^{-3}.

In conclusion, the CR model used in the present paper is a detailed physical model and the atomic data used are adequate for predicting the L-shell emission spectra of calcium. On the whole, the discrepancies of relative intensities between present calculation and experimental measurements are small. The main reason is that the meta-stable state excitation and the cascade effects from the higher excited states (n=3) have been considered in this model. The cascade effects from n=4 and 5 have one order of magnitude fewer effects compared with the cascade effects from n=3. Therefore, the neglect of cascade effects from n=4 and 5 will not have great influence on the electron population density of lower excited states. Because population fractions of every ionization stage as functions of charge state are very sensitive to electron temperature, the derived electron temperature from the theoretical spectra is consistent with the experimental value. In addition, many emission lines from $\Delta n = 0$ of the same ion can be used as diagnostic application for its sensitivity to the electron density. We use three intensity ratios between the five lines from Be-like and C-like calcium ions to determine the electron density. A good agreement between the derived electron density range and the experiment measurement has been found.

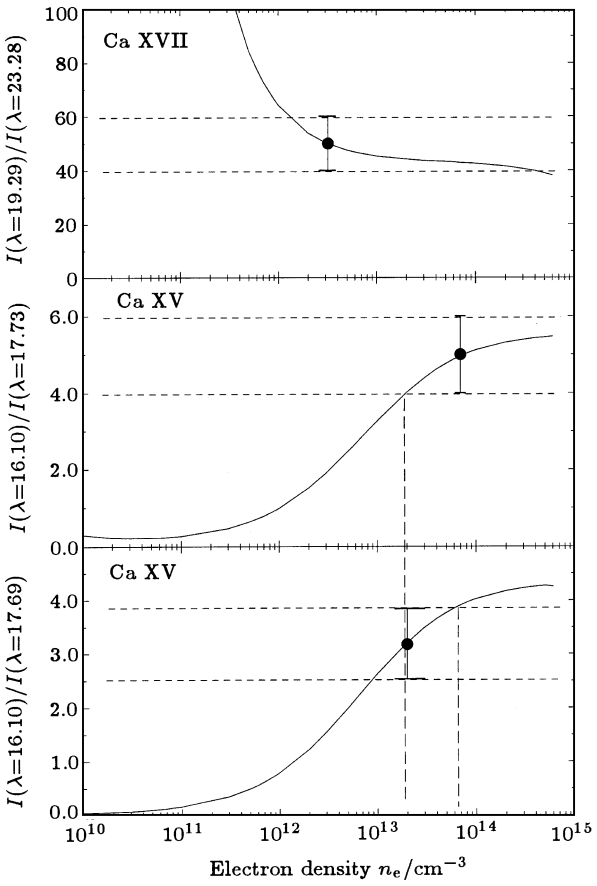


Fig.3. Predicted intensity ratios of the spectral lines of Ca XVII and Ca XV $R_1 = I(2s2p\ ^1P_1\text{–}2s^2\ ^1S_0)/I(2p^2\ ^3P_2\text{–}2s2p\ ^3P_2)$, $R_2 = I(2s2p^3\ ^1D_2\text{–}2s^22p^2\ ^1D_2)/I(2s2p^3\ ^3P_0\text{–}2s^22p^2\ ^3P_1)$ and $R_3 = I(2s2p^3\ ^1D_2\text{–}2s^22p^2\ ^1D_2)/I(2s2p^3\ ^3P_1\text{–}2s^22p^2\ ^3P_1)$ as the function of electron densities at the electron temperature $\log T_e$ (K)=6.745.

References

[1] Porquet D and Dubau J 2000 *Astron. Astrophys. Suppl. Ser.* **143** 495

[2] Porquet D *et al* 2001 *Astron. Astrophys.* **376** 1113

[3] Zeng J L *et al* 2000 *Phys. Rev.* E **62** 7251

[4] Zeng J L, Yuan J M and Lu Q S 2001 *Phys. Rev.* E **64** 66412

[5] Zeng J L, Jin F T, Zhao G and Yuan J M 2003 *Chin. Phys. Lett.* **20** 862

[6] Doschek G A 1990 *Astronphys. J. Suppl. Ser.* **73** 117

[7] Keenan F P *et al* 1998 *Astrophys. J.* **503** 953

[8] Kato T, Fujiwara T and Hanaoka Y 1998 *Astrophys. J.* **492** 822

[9] Lippmann S *et al* 1987 *Astrophys. J.* **316** 819

[10] Soukhanovskii V A *et al* 2000 *Astron. Astrophys. Suppl. Ser.* **142** 95

[11] Yang G H *et al* 2000 *Acta Phys. Sin.* **49** 2389 (in Chinese)

[12] Liu H J *et al* 2002 *Chin. Phys.* **11** 795

[13] Burgess A and Tully J A 1992 *Astron. Astrophys.* **254** 436

[14] Mazzotta P, Mazzitelli G, Colafrancesco S and Vittorio N 1998 *Astron. Astrophys. Suppl. Ser.* **133** 403

[15] Young P R *et al* 2003 *Astrophys. J. Suppl. Ser.* **144** 135

[16] Dere K P *et al* 1997 *Astron. Astrophys. Suppl. Ser.* **125** 149

[17] Zhang H L, Sampson D H and Fontes C J 1990 *At. Data Nucl. Data Tables* **44** 31

[18] Martin I, Karwowski J, Diercksen G H F and Barrientos C 1993 *Astron. Astrophys. Suppl. Ser.* **100** 595

[19] Zhang H L and Sampson D H 1992 *At. Data Nucl. Data Tables* **52** 143

[20] Wiese W L and Fuhr J R 1995 *Atomic Spectra Data Base* (Gaithersdurg: NIST)

[21] Bhatia A K and Doschek G A 1993 *At. Data Nucl. Data Tables* **53** 195

[22] Bhatia A K and Mason H E 1997 *At. Data Nucl. Data Tables* **66** 119

[23] Finkenthal *et al* 1987 *Astrophys. J.* **313** 920